Title
Prolonged survival of transplanted stem cells after ischaemic injury via the slow release of pro-survival peptides from a collagen matrix

Permalink
https://escholarship.org/uc/item/03g9x8xx

Journal
Nature Biomedical Engineering, 2(2)

ISSN
2157-846X

Authors
Lee, Andrew S
Inayathullah, Mohammed
Lijkwan, Maarten A
et al.

Publication Date
2018-02-01

DOI
10.1038/s41551-018-0191-4

Peer reviewed

Prolonged survival of transplanted stem cells after ischaemic injury via the slow release of pro-survival peptides from a collagen matrix

Andrew S. Lee[1,2,3,4,5,7], **Mohammed Inayathullah**[1,4,5,7], **Maarten A. Lijkwan**[1,7], **Xin Zhao**[1,7], **Wenchao Sun**[1,2,3,4,5], **Sujin Park**[1,2,3], **Wan Xing Hong**[1,2,3], **Mansi B. Parekh**[4], **Andrey V. Malkovskiy**[4], **Edward Lau**[1], **Xulei Qin**[1], **Venkata Raveendra Pothineni**[4], **Verónica Sanchez-Freire**[1,2,3], **Wendy Y. Zhang**[1,2,3], **Nigel G. Kooreman**[1,2,3], **Antje D. Ebert**[1,2,3], **Charles K. F. Chan**[2,6], **Patricia K. Nguyen**[1,3,*], **Jayakumar Rajadas**[1,4,5,*], and **Joseph C. Wu**[1,2,3,5,*]

[1]Stanford Cardiovascular Institute, Stanford University School of Medicine, Stanford, CA, USA

[2]Institute for Stem Cell Biology and Regenerative Medicine, Stanford University School of Medicine, Stanford, CA, USA

[3]Department of Medicine, Division of Cardiology, Stanford University School of Medicine, Stanford, CA, USA

[4]Biomaterials and Advanced Drug Delivery Laboratory, Stanford University School of Medicine, Stanford, CA, USA

[5]Pharmacology Division, Stanford University School of Medicine, Stanford, CA, USA

[6]Department of Surgery, Division of Plastic and Reconstructive Surgery, Stanford University School of Medicine, Stanford, CA, USA

Abstract

Stem-cell-based therapies hold considerable promise for regenerative medicine. However, acute donor-cell death within several weeks after cell delivery remains a critical hurdle for clinical translation. Co-transplantation of stem cells with pro-survival factors can improve cell engraftment, but this strategy has been hampered by the typically short half-lives of the factors and

by the use of Matrigel and other scaffolds that are not chemically defined. Here, we report a collagen–dendrimer biomaterial crosslinked with pro-survival peptide analogues that adheres to the extracellular matrix and slowly releases the peptides, significantly prolonging stem cell survival in mouse models of ischaemic injury. The biomaterial can serve as a generic delivery system to improve functional outcomes in cell-replacement therapy.

Capitalizing on their intrinsic ability for self-renewal and on their potential to differentiate into a variety of cell lineages, stem cells have been widely employed for therapeutic applications. Unfortunately, the clinical translation of stem cells has been limited by acute donor-cell death[1,2]. Biomaterials offer a potential niche for the maintenance and precise control of stem cell fate[3–8]. In this study, we aim to significantly improve the in vivo survival of stem cell grafts for regenerative medical applications by enabling the slow release of pro-survival factors conjugated to delivered cells. To identify pro-survival components for use in our biomaterial to treat ischaemic injury, we evaluated a selection of growth factors on the basis of previous studies from our laboratory and others (see Supplementary Table 1)[9–11]. For initial screening, bone marrow mononuclear cells (BMMNCs) were used, given their prevalence in clinical trials and their potential applications to human patients[12]. BMMNCs were harvested from transgenic L2G mice, which constitutively express the firefly luciferase (FLuc) and green fluorescence protein (GFP) reporter genes driven by the β-actin promoter, as previously described (Supplementary Fig. 1a,b)[13]. BMMNCs were co-injected with individual pro-survival factors at separate sites under the dorsum of adult FVB donor mice, and in vivo cell survival was monitored by bioluminescence imaging (BLI) (Supplementary Fig. 1c). BMMNCs co-injected with bone morphogenetic protein-2 peptide analogue (BMP2), erythropoietin peptide analogue (EPO) and fibroblast growth factor-2 peptide analogue (FGF2) were observed to survive longer than cells delivered alone or with other molecules, although all cells were observed to die by day 17 post-injection due to the short half-lives of the BMP2, EPO and FGF2 factors. In vitro lactate dehydrogenase assays confirmed decreased cytotoxicity in BMMNCs cultured under hypoxic conditions when incubated with BMP2, EPO and FGF2 (Supplementary Fig. 1d). Western blot of BMMNCs demonstrated activation of BMP2, EPO and FGF2 recombinant protein activated AKT (protein kinase B, also known as AKT) and mitogen-activated protein kinase/extracellular signal-regulated kinase (MAPK/ERK) pro-survival signalling pathways (Supplementary Fig. 1e)[14]. Dose-dependent activation of AKT and ERK was further detected when cells were treated with the peptides (Supplementary Fig. 2a) as well as upregulation of the anti-apoptotic and pro-survival proteins Hsp70 and Bcl-xL (B-cell lymphoma-extra large) and down-regulation of cleaved caspase 3, indicating a reduced amount of apoptosis (Supplementary Fig. 2b).

Compared with full-length proteins, peptide analogues maintaining the same or partial biological effects may serve as more desirable therapeutic agents because of improved stability, reduced manufacturing cost, fewer side effects and better delivery[15]. To improve the half-life of peptide analogues of BMP2, EPO and FGF2 in vivo as well as the retention of the injected cells, we hypothesized that peptide analogues could be covalently cross-linked to a collagen matrix scaffold via dendrimers (col×D×pep, in which col represents collagen, × represents crosslinked, D represents dendrimer and pep represents peptide) to

provide a controlled delivery system. Specifically, our col×D×pep cocktail contained a combination of BMP2, EPO and FGF2 individually crosslinked to dendrimized collagen (for example, col×D×BMP2, col×D× EPO and col×D× FGF2). Previous studies have employed physical encapsulation, biotin–streptavidin conjugation, click chemistry and other covalent crosslinking methods to enable the slow release of growth factors[16]. However, these studies have largely failed to demonstrate a sustained high level of cell survival in vivo at both early and late stages of delivery or have been non-compatible with Food and Drug Administration standards of human safety[4–6,17–19]. To remedy this shortcoming, we applied a technique to immobilize growth factor peptides on dendrimerzed collagen to produce a stabilized and injectable cell delivery matrix for slow release of pro-survival factors.

Results

Design of the col×D×pep delivery system

To increase the amine functionality on collagen, collagen was crosslinked with first-generation polyamidoamine dendrimers, which are rich in amine groups (Fig. 1a). Dendrimer crosslinking was achieved by coupling the amine groups on dendrimers to the carboxyl groups of collagen's ≈ 12% acidic amino acids (for example, aspartic acid and glutamic acid) through the standard peptide coupling method utilizing 1-ethyl-3-(3-dimethylaminopropyl) carbodiimide and N-hydroxysulfosuccinimide (EDC/sulfo-NHS) to obtain col× D. Pro-survival peptides BMP2, FGF2 and EPO were separately crosslinked to the dendrimers on collagen using the same crosslinkers.

The primary amine content of the collagen was determined via a colorimetric assay using trinitrobenzene sulfonic acid (TNBSA). The amine content was normalized to the collagen concentration, which was determined by a hydroxyproline assay, as described in the Supplementary Information. A significant increase (approximately fivefold) of amine groups was observed after conjugation of dendrimers (Fig. 1b). Collagen samples were further analysed by tris-borate-EDTA–polyacrylamide gel electrophoresis (PAGE), an electrophoresis technique optimized to detect free dendrimers. Prior to dialysis, only traces of free dendrimers were detected, indicating a large extent of crosslinking (Fig. 1c). After dialysis, no free dendrimer was found to migrate into the gel, confirming that the increased amine functionality was due to immobilized dendrimers.

To quantify the amount of pro-survival peptides crosslinked to the collagen in our col×D×p ep delivery system, the amino terminus of the peptides was modified with hexynoic acid (the hexynoyl group contains a carbon–carbon triple bond), which can be quantitatively measured by an azide fluorescent probe using a click chemistry approach (Fig. 1d)[20]. Crosslinking occurred in the range 7–19 nmol peptide/collagen by weight, resulting in an average crosslinking efficiency of 33 ± 12% s.d. (range between 26% and 56%) for all three peptides (Fig. 1e). Peptide crosslinking was further confirmed by sodium dodecyl sulfate (SDS)–PAGE (Fig. 1f). Most of the free peptides were removed after dialysis, as evidenced by the presence of low-molecular-weight peptides (5–10% by densitometry) in the dialysed samples. Self-crosslinking of collagen was identified as a very high-molecular-weight species in the wells of SDS–PAGE (~20% by densitometry). Therefore, we concluded that the signals detected after the click reaction were from peptides that were covalently

immobilized to collagen. Further size-exclusion chromatography (Supplementary Fig. 3) indicated that the col×D and col×D× pep elute at the high-molecular-weight region similar to collagen. The low-molecular-weight species (non-crosslinked peptides) were present at < 5% (see the Supplementary Information for a detailed discussion).

We next examined the secondary structures of collagen in our col×D× pep preparations both with and without linked peptides by circular dichroism (Supplementary Fig. 4). The positive peak at 221 nm was consistent with the triple helix structure of collagen (Supplementary Fig. 4a)[21]. Temperature-dependent circular dichroism spectra of collagen with linked peptides demonstrated the same trend as the control (for example, collagen alone) (Supplementary Fig. 4b). Differential scanning calorimetry further demonstrated that the thermal stability of collagen samples was unaltered when modified with dendrimer and peptides (Supplementary Fig. 4c). Col×D× pep was then analysed by Raman spectroscopy. Investigation of the region characteristic of the amide I band ($1,620$–$1,720$ cm^{-1}) showed that the triple helix conformation was preserved following grafting of dendrimers and linking to peptides even though a decrease in the intensity of the peaks was observed without any peak shift (Supplementary Fig. 5a). The region characteristic of C–H vibrations demonstrated a strong peak around $2,995$ cm^{-1} for the dendrimer-functionalized collagen, which is attributed to the NH_3^+ group in the material (Supplementary Fig. 5b). Another well-known property of collagen I, namely, fibril formation from acid-soluble collagen I monomers, was observed in vitro by raising the pH and temperature of the collagen solution[22]. As quantified by a turbidity assay, unmodified collagen exhibited a typical turbidity curve of increased optical density as collagen fibrils formed (Supplementary Fig. 6). Interestingly, no increase in turbidity was detected for peptide-linked collagen, indicating that crosslinking-stabilized collagen preparations remained in a non-fibrillar form[23]. Dynamic light scattering relaxation curves (Supplementary Fig. 7) showed the absence of a plateau around the time points approaching 1 s, which indicated the presence of large aggregates in the peptide-linked collagen. A plateau below 1,000 μs showed no relaxation, indicating the absence of any individual small particles in solution. The morphology of collagen before and after crosslinking with BMP2, EPO and FGF2 was also examined by scanning electron microscopy. Unmodified collagen showed a fibrous structure, whereas peptide-crosslinked collagens appeared as aggregates (Fig. 1g). Further, atomic force microscopy (Supplementary Fig. 8) showed non-fibrillar structural features that were ≈ 1 nm in height, which excludes the possibility of fibre bundles, indicating the presence of non-fibrillar aggregates.

Gradual release of peptide factors from the colxDxpep delivery system

To test whether covalent conjugation results in a slower release of the peptide analogues, we next compared the release kinetics of crosslinked versus unlinked peptides in a cell-free system by using a one-sided slab at the bottom of a micro centrifuge tube with a phosphate-buffered saline (PBS) layer on top. Peptides were labelled with an azide fluorescent probe using click chemistry for tracking and quantification. Unlinked peptides were rapidly released within the first two to three days when physically mixed with collagen, which is consistent with the short peptide half-lives reported previously in the literature (Fig. 2)[20]. By comparison, cross-linked peptides demonstrated prolonged release lasting for periods longer

than 15 days. A mixture of col× D and free peptide was included as an additional control to examine the effect of dendrimer crosslinking on free-peptide release. Interestingly, dendrimer crosslinking resulted in different release profiles for different peptides, possibly due to the differential alterations in collagen structure and charges (Fig. 2a–c). The slowest release profile, however, was observed only when peptides were covalently crosslinked (Fig. 2d).

Peptides covalently crosslinked are released gradually as collagen degrades and autolysis occurs. The presence of the dendrimer moieties promotes hydrolysis of the amide bonds[24,25], fostering peptide release (Supplementary Fig. 9). Of the two cleavable sites (dendrimer–peptide and dendrimer–collagen), the dendrimer–peptide link has greater exposure to solvent, is more accessible for chemical transformations and is thus more prone to autolysis. After autolytic cleavage, the release kinetics depends on the binding affinity of the peptide to dendrimers in col× D, which varies according to the number of hydrogen donor groups in each peptide. The quicker release of peptides from col× D + peptide compared to col + peptide is probably due to the low binding affinity of peptides to the highly positively charged dendrimers present in col× D (Fig. 2a–c). Of the three peptides in our cocktail, BMP2 and EPO have the lower number of hydrogen bond donor groups in their sequences (Supplementary Fig. 10), resulting in a lower binding affinity and a faster release (Fig. 2a–c). The Raman spectroscopic results also indicate a strong peak around 2,995 cm^{-1}, which is attributed to the NH_3^+ group in col×D× BMP2 and col×D× EPO, indicating higher charge density (Supplementary Fig. 5b). Mass spectrometry (matrix-assisted laser desorption/ionization) was then used to determine the molecular weight of the released peptides (Supplementary Fig. 11a), whose molecular weight was comparable to that of free peptides, as shown by stained SDS–PAGE and fluorescence imaging (Supplementary Fig. 11b,c).

In vivo release kinetics of peptides labelled with an azide fluorescent probe was then assessed by injecting collagen-crosslinked peptides into the hind limbs of severe combined immune-deficient (SCID) mice and explanting the gastrocnemius muscle at defined time points after delivery. As the released peptides are constantly removed (either by consumption or via clearance), the results represent the quantity of the col×D× pep that is present/remaining in the tissue. For non-conjugated preparations, free peptides were observed to fall to low levels as early as ten days after injection (Fig. 2a–c). In contrast, crosslinked preparations yielded detectable levels of free peptide through day 60 post-injection (Fig. 2d). Subcutaneous injection of L2G BMMNCs into the dorsum of SCID mice confirmed that the slow release of growth factors by col×D×pep prolonged cell survival in vivo as compared to BMMNCs receiving unlinked collagen or peptides (Supplementary Fig. 12a–c).

Functional improvements in murine models of hind-limb ischaemia and myocardial infarction

To test the bioavailability and the diffusion of the collagen-based slow release delivery system in vivo, firefly D-luciferin (Luc) was linked to the slow delivery system (col×D× Luc) according to the protocol described in the Supplementary Methods (Supplementary Fig. 13).

Animals were injected with col×D× Luc in the left gastrocnemius muscle, and collagen + Luc or PBS + Luc alone was injected into the right gastrocnemius muscle as a control. BLI was performed at various time points until only background signals were measured (for more detail, see Supplementary Information). These results confirmed that the cross-linked molecules were delivered slowly (Supplementary Fig. 14). Movement or diffusion was also restricted due to the high molecular weight (Supplementary Fig. 11) of the slow-release delivery system and the binding of the collagen element to factors in the extracellular matrix (ECM) (Supplementary Fig. 15), including collagen in the ECM, the fibronectin heparin complex and glycos-aminoglycans (for example, heparin and heparin sulfate)[26]. These interactions helped retain the injected complex for at least 14 days (Supplementary Fig. 14). To study the binding of col×D×pep with ECM, different concentrations of col×D× pep were titrated against chondroitin sulfate, heparin sulfate, hyaluronic acid, collagen IV, collagen I and fibronectin. The results (Supplementary Fig. 16) indicate that the col×D× pep interacts and binds to ECM components.

We next evaluated the pro-survival effects of the col×D×pep slow-release delivery system on BMMNCs in a murine model of hind-limb ischaemia[27]. Preparations of PBS, unlinked peptides or col×D× pep with 1×10^6 BMMNCs were delivered into the right hind limb of SCID mice and immunocompetent mice following unilateral hind-limb ischaemia. Cell survival was monitored by BLI at days 2, 7 and 14 after transplantation. The BLI signal from cells injected with PBS alone or unlinked peptides diminished by day 14, indicating significant cell death as previously reported. By comparison, cells delivered with col×D× pep were found to engraft robustly for the duration of the experiment (Fig. 3a,b). To assess the physiological consequences of the implanted cells and/or materials, limb perfusion was monitored by laser Doppler imaging (Figs. 3c,d and 4). Mice injected with PBS had only low levels of revas-cularization due to spontaneous recovery[27,28]. Mice that received col×D× pep alone or BMMNCs with unlinked peptides demonstrated a mildly improved recovery. In contrast, the injection of cells with the col×D×pep+ cells resulted in marked improvement of perfusion, reaching statistical significance on day 2 post-transplantation as compared to other groups for SCID recipients and day 14 for immunocompetent animals (Figs. 3c,d and 4).

We next aimed to assess whether the col×D×pep slow-release delivery system could be applied to other stem cell populations more relevant to treatment of myocardial infarction. Previous studies have demonstrated the potential of cardiac progenitor cells (CPCs) for cardiac regeneration but suffered from poor survival in the ischaemic heart[29]. We therefore derived CPCs from the hearts of L2G mice and transplanted these cells into the myocardial border zone of SCID mice and immunocompetent mice undergoing ligation of the left anterior descending artery[30]. To ensure that any effects in CPC survival were due to col×D× pep slow release, a number of control preparations were used including: PBS + cells; collagen+cells; free peptides + cells; and collagen + uncrosslinked peptides+cells.

CPCs delivered without pro-survival matrix demonstrated poor survival, with 80% cell loss by day 4 post-injection, and over 90% loss by day 10, matching previously published findings[29]. In contrast, the BLI signal from cells mixed with col×D× pep persisted at extremely robust levels for up to eight weeks following delivery in SCID mice (Fig. 5a,b).

Cells mixed with PBS, collagen alone, free peptides alone or unlinked collagen and peptides failed to show the same effects, indicating that the slow release of peptides is required for prolonged survival. Although cell survival was also prolonged in immunocompetent mice treated with col×D× pep, the improvement was not as robust as seen in the SCID mice (Fig. 5c,d).

Cell engraftment in the border zone of the infarcted myocardium was confirmed by fluorescence dissecting scope analysis of explanted hearts from a subset of animals at day 30 post-cell-injection. GFP expression was detected at robust levels only in the col× D× pep + cells group, but not in other control groups, validating the pro-survival effects of the slow-release peptide delivery system (Fig. 6a). Activation of the AKT and ERK survival signalling pathways in heart tissues by col×D× pep was revealed by immunofluorescence staining several weeks after cell delivery (Fig. 6b). Taken together, these results suggest that collagen crosslinked pro-survival peptides promote long-term survival of CPCs after transplantation into the mouse heart by activating the AKT and ERK pathways.

Next, cardiac function was assessed in treatment groups by echocardiogram and small-animal magnetic resonance imaging (MRI) through eight weeks post-surgery At day 2 post-infarction, echocardiogram demonstrated a significant decrease in fractional shortening for all animals compared with that seen at the baseline, consistent with successful induction of myocardial infarction. At week 2, no significant change was found in any group, probably due to the residual effects of myocardial stunning from acute injury. However, at weeks 4 and 8, SCID animals treated with col×D×pep + cells were found to have a statistically improved left ventricular function as measured by echocardiography (Fig. 6c–e). Although this improvement in cardiac function was observed to persist in immunodeficient mice up to 8 weeks after myocardial infarction, it was maintained in immunocompetent mice only up to 6 weeks post-transplantation (Fig. 7a,b). These findings are consistent with our BLI results above, which demonstrate improved cell survival in SCID mice as compared to immunocompetent mice (Fig. 5). MRI confirmed the improvement in the ejection fraction for SCID animals at weeks 4 and 8 (Fig. 7c,d), as well as left ventricular remodelling at weeks 2, 4 and 8 following myocardial infarction (Fig. 8a). Importantly, histological analysis further corroborated our in vivo imaging results, demonstrating that mice treated with col×D× pep had less infarct and more viable tissue than other treatment groups (Fig. 8b,c).

RNA sequencing confirms col×D×pep activates pro-survival pathways

To confirm that col×D× pep activated pro-survival pathways leading to improvement in cell survival and tissue function, we performed RNA sequencing of CPCs treated with col×D× pep, unlinked collagen + peptide and peptide-only treated samples following a 96 h in vitro incubation. Gene expression analysis suggests that the col×D× pep replicate samples were significantly different from either the unlinked collagen + peptide or the peptide-treated samples, suggesting a synergistic effect on the recipient cell's gene expression from the crosslinking. Pathway analysis of the differential expression data suggests that, compared to collagen + peptide and peptide-only treated samples, treatment with the col×D× pep led to increased expression of genes involved in the mitogen-activated protein kinase (MAPK) and phosphatidylinositol-3-OH kinase–protein kinase B (PI3K–AKT) pro-survival signalling

pathways as well as reduced pro-apoptotic signalling from extracellular stimuli (Supplementary Fig. 17). In particular, expression of multiple genes along the MAPK cascade including harvey rat sarcoma viral oncogene homolog (HRAS), v-raf-1 murine leukemia viral oncogene homolog 1 (RAF1), mitogen-activated protein kinase kinase 1/ mitogen-activated protein kinase kinase 2 (MAP2K1/MAP2K2) and MAPK1 were found to be increased, along with PIK3–AKT signalling genes including phosphoinositide-3-kinase, catalytic, alpha polypeptide (PIK3CA), PIK3CG and PIK3R1, which also showed upregulation. Similarly, two major pro-apoptotic signalling genes TIMP3 and CD28 were observed to be repressed at the transcriptomic level in cells treated with col×D× pep. Taken together, RNA sequencing data suggest that slow release of EPO, BMP2 and FGF2 signalling led to an increase in pro-survival and proliferative pathways and a repression of apoptosis at 96 h post-treatment, consistent with observations from functional studies described in the manuscript.

Discussion

Previous studies have attempted to use biomaterials and/or growth factors in an effort to reduce donor-cell death following in vivo delivery of therapeutic stem cell populations[4,8,18,19,31]. However, these studies have not been able to demonstrate long-term cell survival in the ischaemic microenvironment under chemically defined conditions[19,32,33]. Although Matrigel-based solutions have been identified to promote the survival of cardiomyocytes derived from human embryonic stem cells in infarcted rat hearts[6], the clinical use of Matrigel in human patients is not feasible due to its origination from the ECM of murine Engelbreth–Holm–Swarm sarcoma cells. We therefore excluded the analysis of Matrigel-based preparations from this study and instead focused on the development of a clinically applicable and chemically defined biomaterial for efficient cell transplantation. The col×D× pep pro-survival biomaterial was designed to improve cell engraftment in vivo by combining the advantages of a collagen scaffold with the slow release of pro-survival growth factors. To crosslink the peptides to collagen, we used a conjugation scheme based on a dendrimer-intermediate conjugation. We chose to use a dendrimer because the multi-terminal-free amine groups of the dendrimers increase the limited quantities of amine groups in collagen available for peptide crosslinking and also produce a crosslinked, stable collagen-based material. This crosslinking method enabled us to produce an injectable crosslinked collagen that can be functionalized by different ligands. We have demonstrated that the col×D× pep matrix promotes the engraftment of several types of therapeutic cell in vivo, resulting in functional improvements in animal models of hind-limb ischaemia and myocardial infarction. We anticipate that future studies will improve our understanding of the mechanisms of this pro-survival effect and accelerate its application to the clinic.

Methods

Preparation of peptide-crosslinked collagen. BMP2 mimetic peptide (5hexynoic-KIPKASSVPTELSAISTLYL), EPO mimetic peptide (5hexynoic-GGTYSCHFGPLTWVCKPQGG, disulfide:C6-C15) and FGF2 mimetic peptide (5hexynoic-YRSRKYSSWYVALKRK(YRSRKYSSWYVALKR)-Ahx-Ahx-Ahx-RKRLDRIAR-NH$_2$) were obtained from CS Bio. Acid-soluble collagen I from rat tail (100

mg in 0.02 N acetic acid, ~10 mg ml^{-1}) (BD) was dialysed using 10 K MWCO dialysis cassettes (Thermo Scientific) against 50 mM 2-(*N*-morpholino) ethanesulfonic acid (MES buffer), pH 5.0 at 4 °C. To increase amine functionality, 2.7 ml (molar excess) of polyamidoamine dendrimers (Sigma-Aldrich) mixed with 2.0 ml of MES buffer (pH adjusted to 7.0) was then added to 3 ml of collagen in MES buffer, and was mixed using a 18G needle by gently drawing up and then expelling repeatedly for 10 min at 4 °C. The addition of an excess amount of dendrimers also helped minimize self-crosslinking of collagen. To this mixture, 2 mg of 1-ethyl-3-(3-dimethylaminopropyl) carbodiimide (EDC) (Thermo Scientific) and *N*-hydroxy-sulfosuccinimide (sulfo-NHS) (Thermo Scientific) were added and mixed using a 18G needle for 30 min, and then overnight with a stir bar at 4 °C. The above mixture was then diluted with 3.2 ml of 50 mM MES buffer pH 7.0 and forced through 21G, 26G and 30G needles. Importantly, passing through the needles with different gauges did not affect the crosslinking or the release profile of the material (Supplementary Fig. 18). The treated collagen was then dialysed against 50 mM MES buffer pH 7.0 to remove unreacted dendrimers and crosslinking reagents. For crosslinking of BMP2 and EPO, 3 mg of peptides were dissolved in 0.3 ml dimethyl formamide and activated by mixing with EDC (1 mg) and sulfo-NHS (2 mg) dissolved in 60 µl 50 mM MES pH 5.0 for 30 min at room temperature. After activation, the peptides were purified on a PD mini-trap G10 column (GE Healthcare Life Sciences) and then mixed with 3 ml of dendrimerized collagen at 4 °C for 30 min using a syringe with an 18G needle, and overnight by a stir bar. Peptide-linked collagen was then dialysed against 50 mM MES buffer pH 6.0 to remove unreacted peptides and crosslinking reagents.

Quantification of free amines by TNBSA assay

Primary amine groups of unmodified and crosslinked collagen were determined using the TNBSA assay (Thermo Scientific) according to the manufacturer's instructions. The free amine groups were quantified by comparison to a standard curve of known concentrations of glycine.

Click chemistry and fluorescence assays to quantify peptide using coumarin azide

To quantify the amount of pro-survival peptides crosslinked to the collagen, the N terminus of the peptides was modified with hexynoic acid, which can be quantitatively measured by an azide fluorescent probe using click chemistry. A coumarin azide derivative was used as the probe, which by itself was non-fluorescent due to the quenching effect from the electron-rich α-nitrogen of the azido group. On click reaction, the quenching effect is released, yielding a fluorescent signal proportional to the amount of peptide. A volume of 12.5 µl of 2 mM 3-azido-7-hydroxycoumarin (Glen Research) dissolved in dimethyl formamide, a premixed solution of 12.5 µl of 5 mM CuSO$_4$ in H$_2$O and 12.5 µl of 5 mM tris(benzyltriazoylmethyl)amine (TBTA) (Sigma) dissolved in dimethylsulfoxide, and 25µl of 100 mM sodium ascorbate (Sigma) in H$_2$O were added to the free and crosslinked peptide samples. The total volume was then brought up to 250 µl. The pH was adjusted to 4.0 using 1 N HCl. The reaction mixture was incubated at room temperature in the dark for 1 h. Fluorescence intensity was measured using a GloMax-Multi micro-plate reader (Promega) with an ultraviolet optical kit (excitation 365 nm, emission 410–460 nm). The concentration

of peptides was calculated by comparison to a standard curve of known concentrations of propargyl alcohol.

In vitro peptide release assay

Two hundred microlitres of collagen with crosslinked or uncrosslinked peptides was deposited at the bottom of a 1.5 ml micro centrifuge tube. After incubation at 37 °C for 15 min, 500 μl of 1×PBS was carefully layered on top of the collagen. The mixture was then incubated at 37 °C for up to 15 days. One hundred microlitres of solution was withdrawn from the PBS layer at different time points and replenished with 100 μl of fresh 1×PBS. Peptides released into the supernatant were quantified by fluorescent labelling using click chemistry, as described above.

In vivo peptide release assay

The hind-limb gastrocnemius muscle of SCID mice was explanted at the various time points after the injection of col×D×pep. The tissue was homogenized in 300 μl of PBS to extract the peptides into the solution. The homogenate was centrifuged at 5,000g for 10 min. The peptides present in the supernatant were quantified by fluorescent labelling using click chemistry, as described above.

Isolation and culture of CPCs

Animal protocols were approved by the Stanford University Animal Care and Use Committee. CPCs were isolated from L2G85 transgenic mice of FVB background with a β-actin promoter driving FLuc-eGFP, as previously described[29]. Briefly, hearts were explanted, cut into 1–2 mm pieces, and digested with 0.1% collagenase II for 30 min at 37 °C while on a shaker. Cells were then filtered through a 100-μm strainer and cultured in Iscove's modified Dulbecco's medium (IMDM) supplemented with 10% fetal bovine serum (FBS) (Hyclone), 0.1 mM non-essential amino acids, 100 U ml^{-1} penicillin G, 100 μg ml^{-1} streptomycin, 2 mM glutamine and 0.1 mM β-mercaptoethanol. After three weeks of culture, a population of phase-bright cells was observed to appear over the adherent cells. Phase-bright cells were collected by light digestion with a cell dissolution buffer (Life Technologies) at room temperature under microscope monitoring, and sub-cultured in poly-lysine-coated plates (BD Biosciences) with the same medium.

Myocardial infarction and cell delivery

SCID Beige mice (Charles River Laboratories) were stratified into one of five groups ($n = 12$ per group), each receiving an intramyocardial injection of CPCs suspended in different solutions as listed: 30 μl of PBS, 30 μl of unmodified collagen I (5 mg ml^{-1} in 50 mM MES pH 6.0), 30 μl of a mixture of BMP2, EPO and FGF2 (0.3 mg ml^{-1} each in a 1:10 solution of dimethylsulfoxide/PBS), 30 μl of an admixture of collagen and peptides (same concentrations as above) or 30 μl of 1:1 col×D×pep/collagen (at a final concentration of 5 mg ml^{-1} in MES pH 6.0 for each). Heparin (Sigma) was also added 1:100 to the groups that contain collagen. For the study of cardiac function, myocardial infarction was induced by aseptic lateral thoracotomy and ligation of the left anterior descending coronary artery, as previously described[34].

Bioluminescence imaging to monitor survival of transplanted cells in living mice

BLI was performed using the Xenogen IVIS 200 in vivo imaging system (Alameda). After intraperitoneal injections of the reporter probe d-luciferin (250 mg of luciferin kg^{-1}), the animals were imaged with exposure times ranging from 2 s to 2 min pre-surgery and followed at days 1, 2, 4, 7 and 14, and weekly thereafter to day 56 post-surgery ($n = 6$ per group). Immunocompetent FVB animals were imaged weekly until day 42 post-surgery ($n = 6$ per group). Imaging signals were quantified in units of maximum photons per second per square centimetre per steradian ($p\ s^{-1}\ cm^{-2}\ sr^{-1}$), as previously described[35].

Immunofluorescence staining

Immunofluorescence stains were performed using primary antibodies phospho-AKT and phospho-ERK1/2 (Cell Signaling Technology) and AlexaFluor-conjugated secondary antibodies (Invitrogen), as previously described[36]. 4′,6-diamidino-2-phenylindole (DAPI) was used for nuclear counterstaining.

Hind-limb ischaemia model

Hind-limb ischaemia was induced in SCID and immunocompetent FVB animals, as previously described[27]. Briefly, mice were anaesthetized with 1.5% isoflurane and the right hind limb was opened to expose the femoral artery for ligation, after which 1×10^6 BMMNCs were delivered into the gastrocnemius muscle using a 29G Hamilton syringe ($n = 5$ per group). Control animals received PBS alone. Skin was closed using 6-0 silk sutures. Following surgery, cell survival and revascularization were monitored by BLI and Doppler perfusion imaging, respectively. Animal studies were approved by the Administrative Panel on Laboratory Animal Care (APLAC) at Stanford University.

Measurement of hind-limb blood flow by laser Doppler imaging

Animals were sedated using 1.5% isoflurane in oxygen, and hind-limb vascularization was monitored by laser Doppler perfusion imaging using a PeriScan PIM3 laser Doppler system (Perimed AB), as described previously for both SCID and immunocompetent FVB animals ($n = 5$ per group)[27]. Temperature variability was maintained at constant levels by keeping animals on heat pads set to 37 °C during measurement. Non-ligated contra-lateral hind limbs served as controls. Perfusion was calculated as the ratio of the flow in the ischaemic to non-ischaemic limbs.

Left ventricular functional analysis with echocardiogram

Echocardiography was performed using a Siemens-Acuson Sequoia C512 system (Malvern) equipped with a multi-frequency (8-14 MHz) 15L8 transducer. SCID mice were assessed at days 2, 14, 28 and 56 post-surgery ($n = 6$ per group). Immunocompetent FVB mice were assessed at days 2, 14, 28, 42 and 56 ($n = 6$ per group). Briefly, animals were sedated using 1.5% inhaled isoflurane and imaged in the supine position. The following formula was used to calculate fractional shortening from M-mode short-axis images of the left ventricle: FS = (left ventricular end-diastolic dimension – left ventricular end-systolic dimension)/(left ventricular end-diastolic dimension).

Assessment of cardiac contractility and left ventricle remodelling with magnetic resonance imaging (MRI)

A subset of SCID mice was assessed by MRI for cardiac function ($n = 6$ per group) at days 2 and weeks 2, 4 and 8 post-surgery using a Signa 3.0 T Excite HD scanner (GE) equipped with a Mayo Clinic T/R MRI coil (Mayo Clinic Medical Devices), as previously described. Briefly, mice were sedated using 1.5% isoflurane with 1 ml min^{-1} of oxygen, and murine electrocardiogram, respiration and body temperature were monitored (Small Animal Instruments). Gradient-recalled echo was employed for cardiac localization, after which 20 short-axis cine frames were acquired using fast spoiled gradient-recalled echo over 1 complete cardiac cycle. The following imaging parameters were applied: TR = 10 ms, TE = 4.6 ms, number of excitations (NEX) = 10, field of view (FOV) = 40×40 mm, matrix = 256×256, flip angle (FA) = 45°, slice thickness 1.5 mm, spacing = 0 mm, imaging voxel size: 1.57×1.57 mm. A commercial contour analysis program (Osirix Version 3.81) was used to calculate ejection fraction by tracing the endocardial border of the left ventricle at end diastole and end systole.

Statistical analysis

Continuous variables with normal distribution were expressed as mean ± s.d. Differences in continuous variables were compared using a one-way analysis of variance (ANOVA) or two-way repeated ANOVA, followed by a Student's t-test. A post-hoc Sidak-Bonferroni correction was performed if needed to adjust for multiple comparisons. Statistical analysis was performed using GraphPad Prism. Tests that had an alpha level for significance set at $P < 0.05$ were considered significant.

Life Sciences Reporting Summary

Further information on experimental design is available in the Life Sciences Reporting Summary.

Data availability

The data that support the findings of this study are available within the paper and its Supplementary Information. All data generated in this study are available from the corresponding authors upon reasonable request. RNA-sequencing data have been deposited into the Sequence Read Archive (SRA): https://www.ncbi.nlm.nih.gov/bioproject/PRJNA412785.

Supplementary Material

Refer to Web version on PubMed Central for supplementary material.

Acknowledgments

References

1. Nguyen PK, Neofytou E, Rhee JW, Wu JC. Potential strategies to address the major clinical barriers facing stem cell regenerative therapy for cardiovascular disease: a review. JAMA Cardiol. 2016; 1:953–962. [PubMed: 27579998]

2. Zwetsloot PP, et al. Cardiac stem cell treatment in myocardial infarction: a systematic review and meta-analysis of preclinical studies. Circ Res. 2016; 118:1223–1232. [PubMed: 26888636]

3. Discher DE, Mooney DJ, Zandstra PW. Growth factors, matrices, and forces combine and control stem cells. Science. 2009; 324:1673–1677. [PubMed: 19556500]

4. Pompe T, Salchert K, Alberti K, Zandstra P, Werner C. Immobilization of growth factors on solid supports for the modulation of stem cell fate. Nat Protoc. 2010; 5:1042–1050. [PubMed: 20539280]

5. Hu S, et al. Novel microRNA prosurvival cocktail for improving engraftment and function of cardiac progenitor cell transplantation. Circulation. 2011; 124:S27–S34. [PubMed: 21911815]

6. Laflamme MA, et al. Cardiomyocytes derived from human embryonic stem cells in pro-survival factors enhance function of infarcted rat hearts. Nat Biotechnol. 2007; 25:1015–1024. [PubMed: 17721512]

7. Seif-Naraghi SB, et al. Safety and efficacy of an injectable extracellular matrix hydrogel for treating myocardial infarction. Sci Transl Med. 2013; 5:173.

8. Cha C, Liechty WB, Khademhosseini A, Peppas NA. Designing biomaterials to direct stem cell fate. ACS Nano. 2012; 6:9353–9358. [PubMed: 23136849]

9. Hahn JY, et al. Pre-treatment of mesenchymal stem cells with a combination of growth factors enhances gap junction formation, cytoprotective effect on cardiomyocytes, and therapeutic efficacy for myocardial infarction. J Am Coll Cardiol. 2008; 51:933–943. [PubMed: 18308163]

10. Zhang Y, Alexander PB, Wang XF. TGF-beta family signaling in the control of cell proliferation and survival. Cold Spring Harb Perspect Biol. 2017; 9:1–22.

11. Hu X, et al. A large-scale investigation of hypoxia-preconditioned allogeneic mesenchymal stem cells for myocardial repair in nonhuman primates: paracrine activity without remuscularization. Circ Res. 2016; 118:970–983. [PubMed: 26838793]

12. Nguyen PK, Rhee JW, Wu JC. Adult stem cell therapy and heart failure, 2000 to 2016: a systematic review. JAMA Cardiol. 2016; 1:831–841. [PubMed: 27557438]

13. Sheikh AY, et al. In vivo functional and transcriptional profiling of bone marrow stem cells after transplantation into ischemic myocardium. Arterioscler Tromb Vasc Biol. 2012; 32:92–102.

14. Muraski JA, et al. Pim-1 regulates cardiomyocyte survival downstream of Akt. Nat Med. 2007; 13:1467–1475. [PubMed: 18037896]

15. Penchala SC, et al. A biomimetic approach for enhancing the in vivo half-life of peptides. Nat Chem Biol. 2015; 11:793–798. [PubMed: 26344696]

16. Vo TN, Kasper FK, Mikos AG. Strategies for controlled delivery of growth factors and cells for bone regeneration. Adv Drug Deliv Rev. 2012; 64:1292–1309. [PubMed: 22342771]

17. Dingal PC, Discher DE. Combining insoluble and soluble factors to steer stem cell fate. Nat Mater. 2014; 13:532–537. [PubMed: 24845982]

18. Burdick JA, Mauck RL, Gerecht S. To serve and protect: hydrogels to improve stem cell-based therapies. Cell Stem Cell. 2016; 18:13–15. [PubMed: 26748751]

19. Davis ME, et al. Local myocardial insulin-like growth factor 1 (IGF-1) delivery with biotinylated peptide nanofibers improves cell therapy for myocardial infarction. Proc Natl Acad Sci USA. 2006; 103:8155–8160. [PubMed: 16698918]

20. Meghani NM, Amin HH, Lee BJ. Mechanistic applications of click chemistry for pharmaceutical drug discovery and drug delivery. Drug Discov Today. 2017; 22:1604–1619. [PubMed: 28754291]

21. Drzewiecki KE, Grisham DR, Parmar AS, Nanda V, Shreiber DI. Circular dichroism spectroscopy of collagen fibrillogenesis: a new use for an old technique. Biophys J. 2016; 111:2377–2386. [PubMed: 27926839]

22. Hubbell JA. Cellular matrices: physiology in microfluidics. Nat Mater. 2008; 7:609–610. [PubMed: 18654581]

23. Zhu JL, Kaufman LJ. Collagen I self-assembly: revealing the developing structures that generate turbidity. Biophys J. 2014; 106:1822–1831. [PubMed: 24739181]

24. Jin E, et al. Acid-active cell-penetrating peptides for in vivo tumor-targeted drug delivery. J Am Chem Soc. 2013; 135:933–940. [PubMed: 23253016]

25. Xu P, et al. Targeted charge-reversal nanoparticles for nuclear drug delivery. Angew Chem Int Ed Engl. 2007; 46:4999–5002. [PubMed: 17526044]

26. Lee SS, et al. Sulfated glycopeptide nanostructures for multipotent protein activation. Nat Nanotechnol. 2017; 12:821–829. [PubMed: 28650443]

27. Niiyama H, Huang NF, Rollins MD, Cooke JP. Murine model of hindlimb ischemia. J Vis Exp. 2009; 23:e1035.

28. Hu S, et al. Effects of cellular origin on differentiation of human induced pluripotent stem cell-derived endothelial cells. JCI Insight. 2016; 1:e85558. [PubMed: 27398408]

29. Li Z, et al. Imaging survival and function of transplanted cardiac resident stem cells. J Am Coll Cardiol. 2009; 53:1229–1240. [PubMed: 19341866]

30. Smith RR, et al. Regenerative potential of cardiosphere-derived cells expanded from percutaneous endomyocardial biopsy specimens. Circulation. 2007; 115:896–908. [PubMed: 17283259]

31. Lutolf MP, Gilbert PM, Blau HM. Designing materials to direct stem-cell fate. Nature. 2009; 462:433–441. [PubMed: 19940913]

32. Kutschka I, et al. Collagen matrices enhance survival of transplanted cardiomyoblasts and contribute to functional improvement of ischemic rat hearts. Circulation. 2006; 114:I167–I173. [PubMed: 16820568]

33. Kraehenbuehl TP, et al. Human embryonic stem cell-derived microvascular grafts for cardiac tissue preservation after myocardial infarction. Biomaterials. 2011; 32:1102–1109. [PubMed: 21035182]

34. Simpson D, Liu H, Fan TH, Nerem R, Dudley SC Jr. A tissue engineering approach to progenitor cell delivery results in significant cell engraftment and improved myocardial remodeling. Stem Cells. 2007; 25:2350–2357. [PubMed: 17525236]

35. Cao F, et al. In vivo visualization of embryonic stem cell survival, proliferation, and migration after cardiac delivery. Circulation. 2006; 113:1005–1014. [PubMed: 16476845]

36. Sun N, et al. Feeder-free derivation of induced pluripotent stem cells from adult human adipose stem cells. Proc Natl Acad Sci USA. 2009; 106:15720–15725. [PubMed: 19805220]
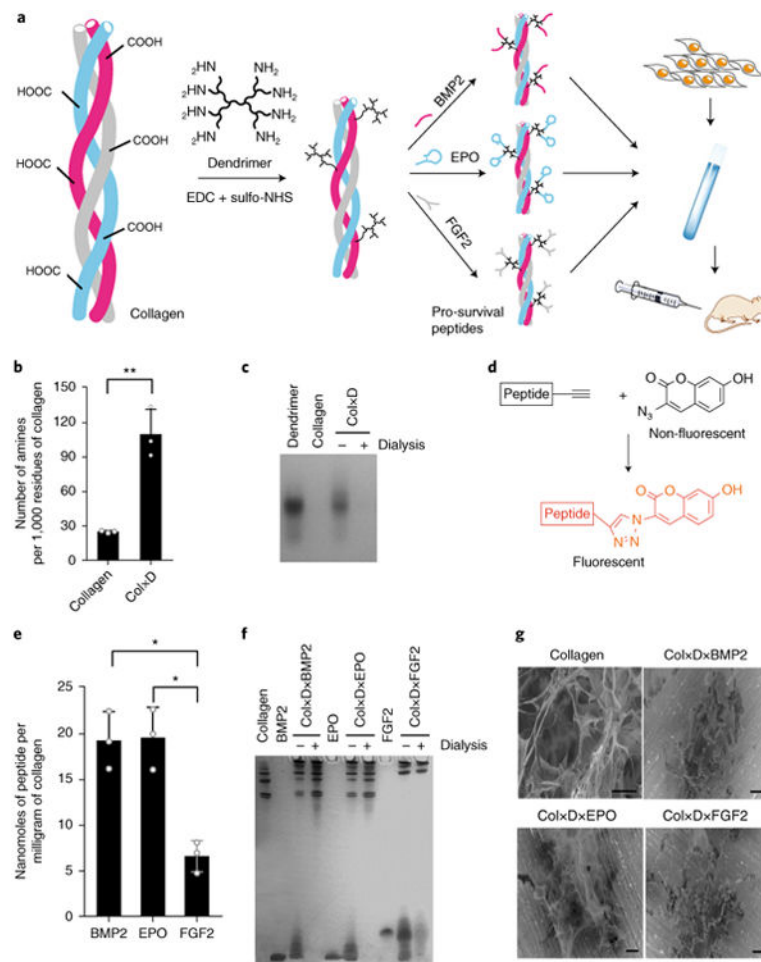
Fig. 1. Preparation of peptide-linked collagen

a, A schematic depicting the method of col×D×pep synthesis. b, Quantification of amine groups on collagen before and after crosslinking using the TNBSA assay. The results are normalized to collagen concentration and expressed as the number of amines per 1,000 residues of collagen (mean ± s.d., $n = 3$). **$P < 0.01$. **c**, Tris-borate-EDTA-PAGE to detect free dendrimers. **d**, A click reaction scheme showing the fluorescent labelling of acetylene-labelled peptides with an azide probe. **e**, Quantification of peptides crosslinked to collagen by click chemistry. The results are normalized to collagen concentration and expressed as nanomoles of peptide per milligram of collagen (mean ± s.d., $n = 3$). *$P < 0.05$. **f**, SDS-PAGE to detect collagen and free peptides. **g**, Scanning electron microscope images of crosslinked collagens. Scale bars, 25 µ m. Distinct samples were measured and the experiments were performed in triplicate.
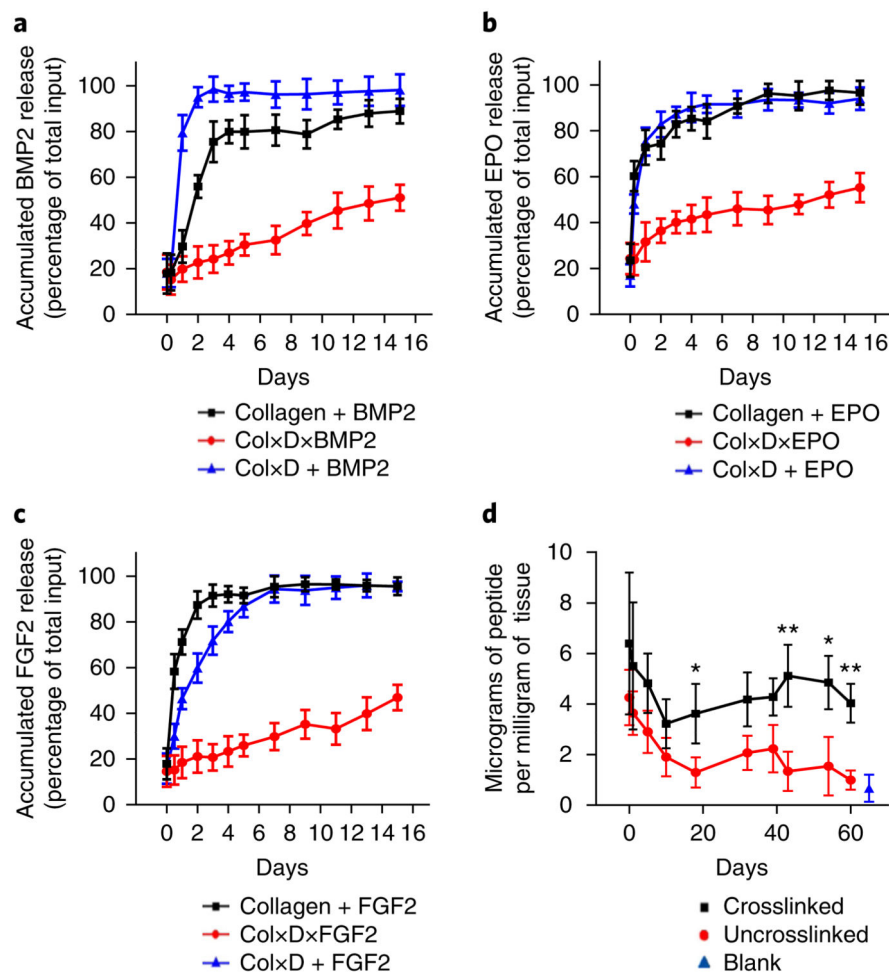
Fig. 2. Slow release of peptides from the col×D×pep pro-survival matrix in vitro and in vivo
a–c, In vitro peptide release of BMP2 (**a**), EPO (**b**) and FGF2 (**c**). Peptide-crosslinked collagen was deposited in a test tube and covered by a layer of 1× PBS buffer. The amount of released peptide was determined by fluorescent labelling using click chemistry. The admixture of free peptides with collagen or dendrimerized collagen was tested as controls. The results are normalized to total peptide input and shown as accumulated release. **d**, For in vivo peptide release, peptide-crosslinked collagen was injected into the hind limbs of SCID mice. The gastrocnemius muscle was then explanted at the indicated time points after delivery for assessment of released peptides by extraction and fluorescent labelling using the click chemistry approach. In **a–c**, the differences are significant between collagen + peptide and col×D× pep at all time points. Each data point is the mean ± s.d., $n = 3$, $P < 0.05$; in **d**, the difference is significant between crosslinked and uncrosslinked peptides; a blank (for example, saline injected) served as a control to measure the background signal. Each data point is mean ± s.d., $n = 3$. *$P < 0.05$; **$P < 0.001$. Distinct samples were measured and experiments were performed in triplicate.
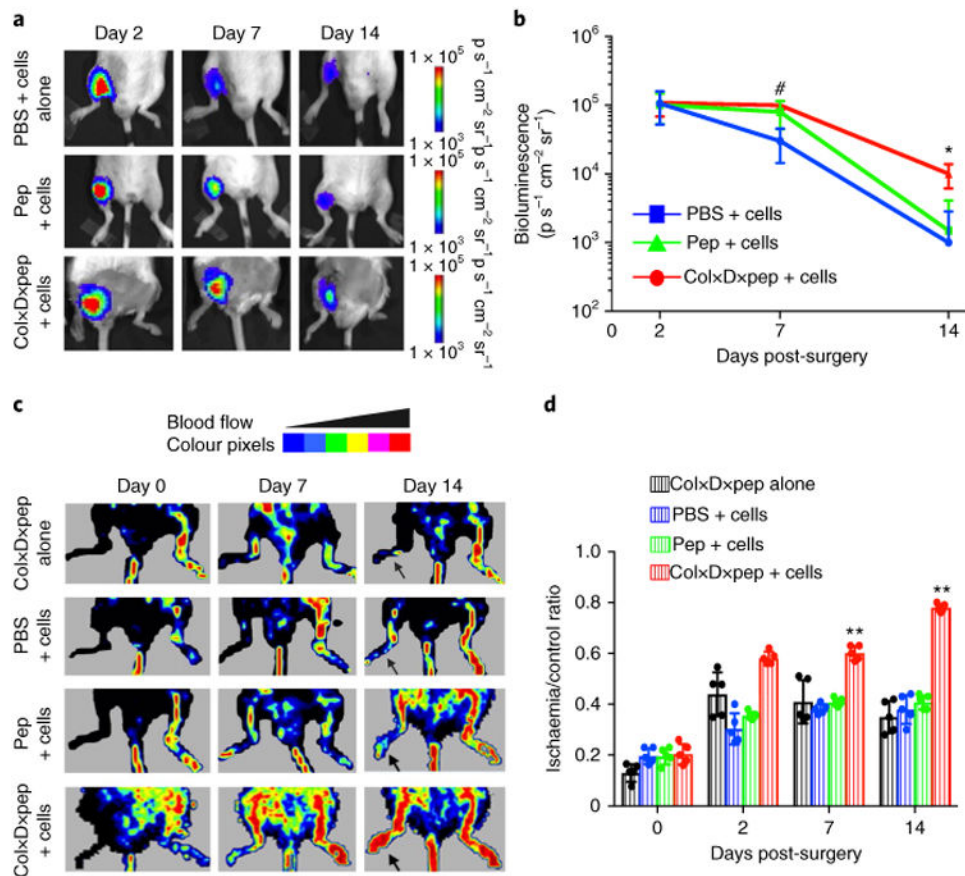
Fig. 3. Evaluation of cell survival and limb perfusion after implanting BMMNCs with col×D×pep in SCID and immunocompetent mice after femoral artery ligation

a, Representative BLI of SCID mice ($n = 5$ per group) after hind-limb injection of BMMNCS with PBS + cells, peptide + cells or col×D×pep + cells treatment groups. **b**, Quantification of BLI. The results are mean ± s.d. ($n = 5$ for all groups). #$P < 0.05$ col×D×pep + cells versus PBS alone; *$P < 0.05$ col×D×pep + cells compared to PBS and peptide + cells. Distinct samples were measured and experiments were performed in duplicate. **c**, Representative laser Doppler images for the col×D× pep alone, PBS + cells, peptide + cells and col×D×pep + cells treatment groups. The arrows indicate the ischaemic limb on day 14 in different groups. **d**, Quantification of blood flow as determined by laser Doppler imaging. Results are mean±s.d. ($n = 5$ for all groups). **$P < 0.01$ compared to all groups.

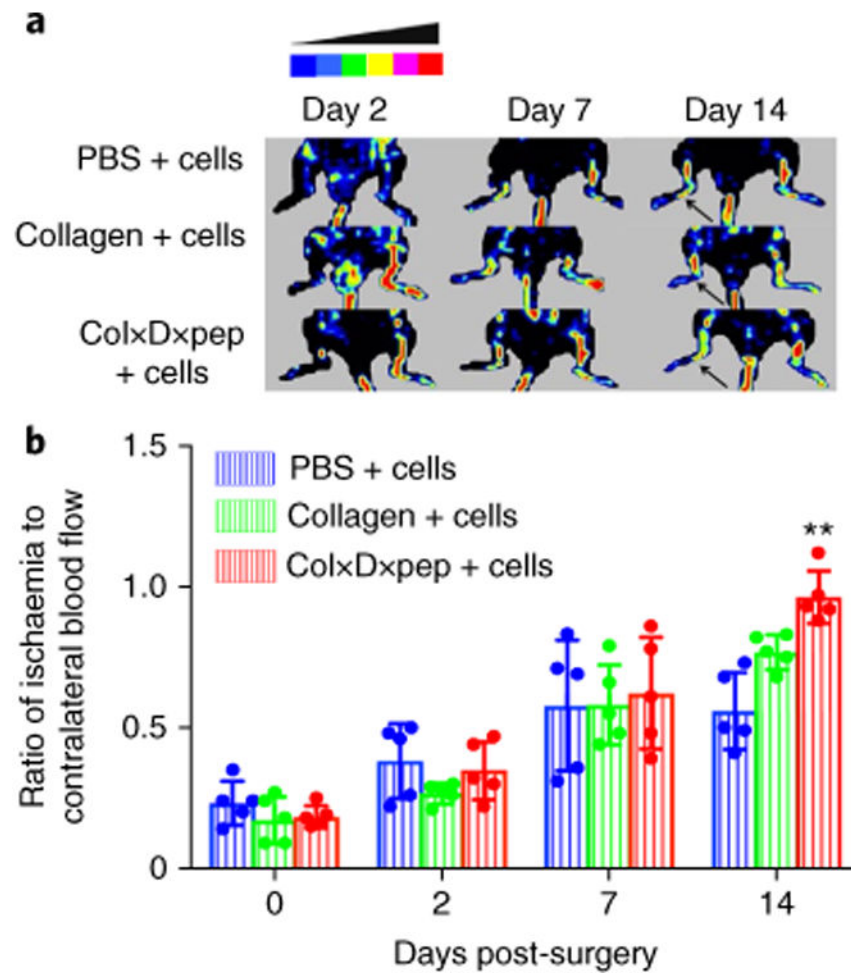**Fig. 4. Evaluation of limb perfusion after implanting BMMNCs with col×D×pep in immunocompetent mice after femoral artery ligation**

a, Representative laser Doppler images for PBS + cells, collagen + cells and col×D×pep + cells treatment groups. The arrows indicate the ischaemic limb on day 14 in different groups.

b, Quantification of blood flow as determined by laser Doppler imaging. The results are mean ± s.d. ($n = 5$ for all groups). **$P < 0.01$ compared to PBS and col×D×pep groups.
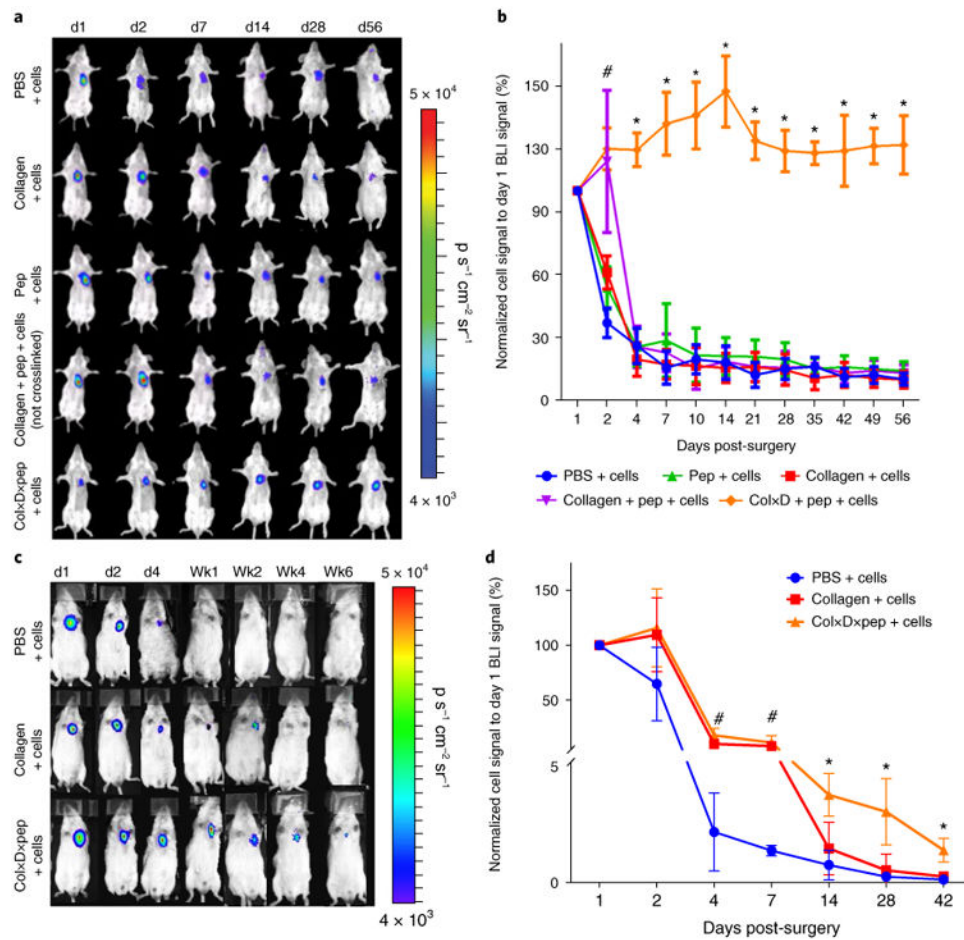
Fig. 5. The col×D×pep pro-survival matrix promotes long-term cell survival in vivo

a, Representative bioluminescence images of SCID mice ($n = 6$ per group) after intra-myocardial injection of CPCs mixed with PBS, unmodified collagen, free peptides, admixture of collagen and free peptides, or col×D× pep cocktail as indicated. **b**, Quantification of BLI signals. The signals for each mouse are normalized to the value on day 1 post-injection. The results are presented as percentage of day 1 (mean ± s.d., $n = 6$, #P < 0.05 col×D×pep + cells versus all other groups except collagen +peptide + cells, *P<0.01 col×D×pep + cells versus all other groups). **c**, Representative bioluminescence images of immunocompetent mice ($n = 6$ per group) after intra-myocardial injection of CPCs mixed with PBS, unmodified collagen or col×D× pep cocktail as indicated. **d**, Quantification of BLI signals. The signals for each mouse are normalized to the value on day 1 post-injection. The results are presented as percentage of day 1 (mean ± s.d., $n = 6$); #P < 0.05 col×D×pep + cells versus all other groups except collagen + peptide + cells. *P < 0.05 col×D×pep + cells versus all other groups.
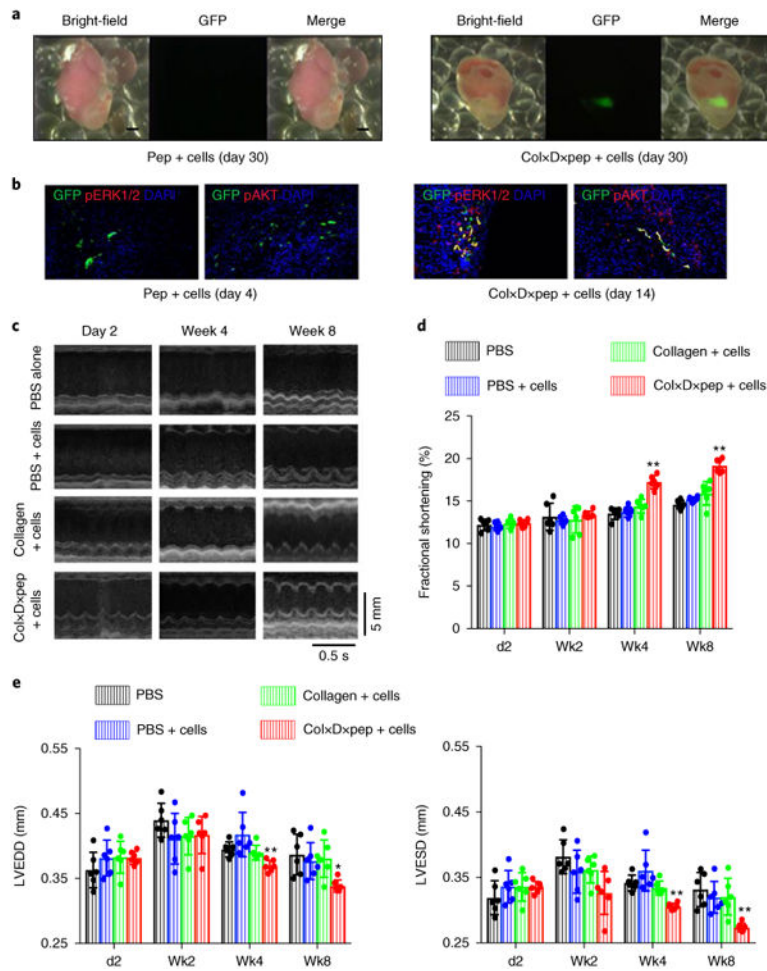
Fig. 6. Evaluation of graft function after implanting cardiac progenitor cells with col×D×pep in a SCID model of myocardial infarction

a, GFP signals (overlaid with a bright-field image) from representative hearts harvested from mice 30 days post-injection. Scale bars, 1 mm. **b**, Immunofluorescence staining of heart tissues for phosphorylated ERK1/2 and AKT. Four days post-injection for cells + peptide group; 14 days post-injection for cells + col×D× pep. The effect of treatment with col×D× pep was statistically different from those for other treatment groups at all time points. **c**, Representative M-mode echocardiographic data for infarcted hearts receiving 1×10^6 CPCs mixed with PBS, collagen alone or col×D× pep. Mice receiving PBS served as a control. **d**, Comparison of fractional shortening. The results are mean ± s.d. ($n = 6$ per group). $**P < 0.01$, $*P < 0.05$ compared to all control groups. **e**, Comparison of the left ventricular end-diastolic dimension (LVEDD) and the left ventricular end-systolic dimension (LVESD). The results are mean ± s.d. ($n = 6$ per group). $**P < 0.01$, $*P < 0.05$ compared to all control groups.
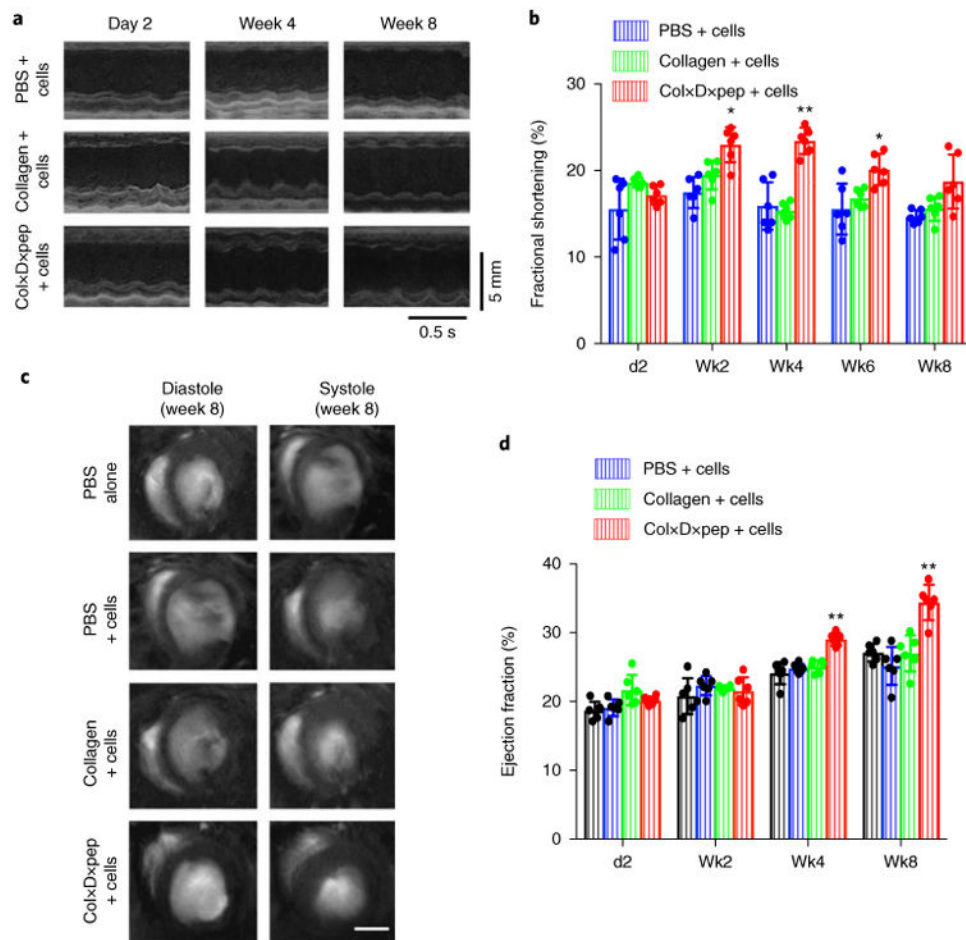
Fig. 7. Evaluation of the effects of CPC delivery with col×D×pep pro-survival matrix on post-infarct ventricular function by echocardiography and MRI

a, Representative M-mode echocardiographic data for infarcted hearts in immunocompetent FVB animals receiving 1×10^6 CPCs mixed with PBS, collagen alone or col×D×pep. **b**, Comparison of fractional shortening. The results are mean±s.d. ($n = 6$ for all groups). **P<0.01, *P< 0.05 compared to all control groups. **c**, Representative short-axis MRI images show hearts receiving PBS alone, CPCs mixed with PBS, CPCs mixed with collagen or CPCs mixed with col×D× pep in immunocompromised mice. The hearts are shown at end-diastole and end-systole. Scale bar, 1 mm. **d**, Quantitative MRI assessments of the left ventricular ejection fraction of infarcted mice. The results are mean±s.d. ($n = 6$ for all groups). **P< 0.01 compared to other groups.
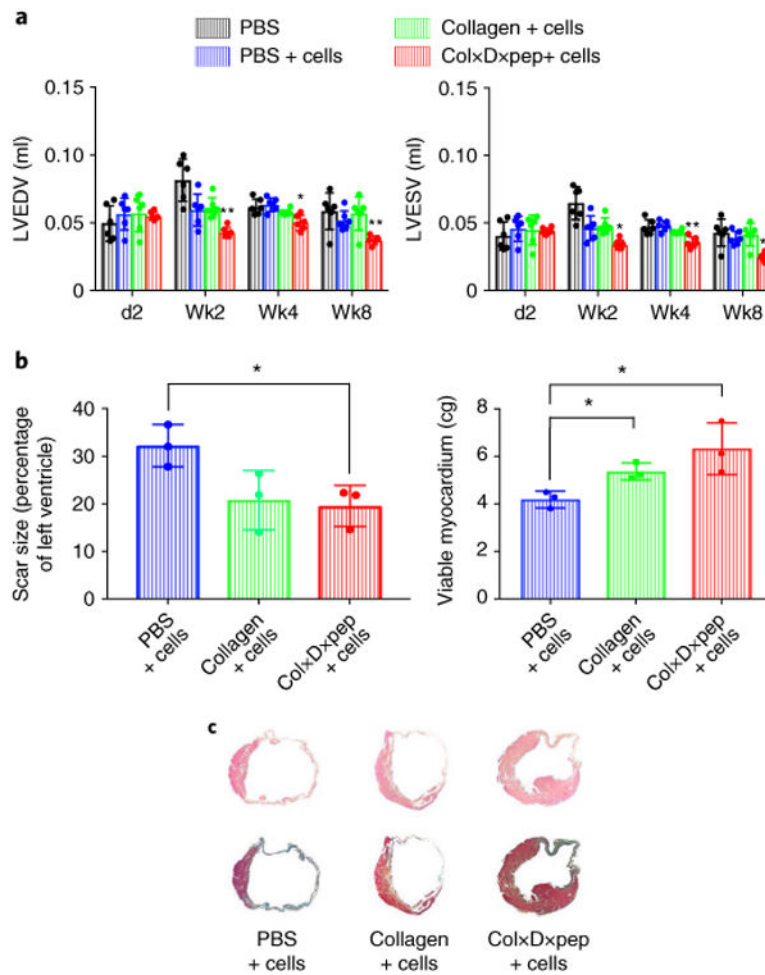
Fig. 8. Evaluation of left ventricular remodelling in immunodeficient mice by MRI after delivery of col×D×pep

a, Quantitative MRI assessments of the left ventricular end-diastolic volume (LVEDV) and the left ventricular end-systolic volume (LVESV) of infarcted mice. The results are mean ± s.d. ($n = 6$ for all groups). **$P < 0.01$, *$P < 0.05$ compared to other groups. **b**, Quantification of the amount of scar and viable tissue by histology. The data are mean ± s.d., $n = 3$. *$P < 0.05$. Distinct samples were measured and experiments were performed in triplicate. **c**, Representative haematoxylin and eosin (top) and Masson's trichrome (bottom) staining of left ventricular tissue of mice receiving CPCs mixed with PBS, collagen alone or col×D× pep. Blue on the Masson's trichrome tissue signifies scar tissue.